Unsteady Reynolds Averaged Navier-Stokes: toward accurate predictions in Fuel- Bundles and T-junctions

E. Merzari, H. Ninokata
Department of Nuclear Engineering,
Tokyo Institute of Technology
Meguro-ku, Ookayama 2-12-2, N1-5 458,
Tokyo, Japan
merzari@nr.titech.ac.jp

E.Baglietto
CD-adapco, New York
60 Broadhollow Rd. Melville, NY 11747

Abstract

Traditional steady-state simulation and turbulence modelling are not always reliable. Even in simple flows, the results can be not accurate when particular conditions occur. Examples are buoyancy, flow oscillations, and turbulent mixing.
Often, unsteady simulations are necessary, but they tend to be computationally not affordable. The Unsteady Reynolds Averaged Navier-Stokes (URANS) approach holds promise to be less computational expensive than Large Eddy Simulation (LES) or Direct Numerical Simulation (DNS), reaching a considerable degree of accuracy. Moreover, URANS methodologies do not need complex boundary formulations for the inlet and the outlet like LES or DNS.
The Test cases for this methodology will be Fuel Bundles and T-junctions. Tight-Fuel Rod-Bundles present large scale coherent structures than cannot be taken into account by a simple steady-state simulation. T-junctions where a hot fluid and a cold fluid mix present temperature fluctuations and therefore thermal fatigue. For both cases the capacity of the methodology to reproduce the flow field are assessed and it is evaluated that URANS holds promise to be the industrial standard in nuclear engineering applications that do not involve buoyancy. The codes employed are STAR-CD 3.26 and 4.06.

Keywords

Thermal Hydraulics, T-junction, CFD, URANS, Tight-Lattice

1. INTRODUCTION

The Navier-Stokes equations in Cartesian coordinates are:

$$\frac{\partial u_i}{\partial t} + u_i \frac{\partial u_i}{\partial x_j} = -\frac{1}{\rho}\frac{\partial (p)}{\partial x_i} - \frac{\partial}{\partial x_j}\left(\nu \frac{\partial u_i}{\partial x_j}\right) \tag{1.1}$$

$$\frac{\partial u_i}{\partial x_i} = 0 \tag{1.2}$$

When ensemble averaging is performed they become the URANS equations:

$$\frac{\partial \langle u_i \rangle}{\partial t} + \langle u_j \rangle \frac{\partial \langle u_i \rangle}{\partial x_j} = -\frac{1}{\rho}\frac{\partial (\langle p \rangle)}{\partial x_i} - \frac{\partial}{\partial x_j}\left(\tau_{ij} - \nu \frac{\partial \langle u_i \rangle}{\partial x_j}\right) \tag{2.1}$$

$$\frac{\partial \langle u_i \rangle}{\partial x_i} = 0 \tag{2.2}$$

Where $\tau_{ij} = \langle u_i u_j \rangle - \langle u_i \rangle \langle u_j \rangle$ needs closure. Please note that ensemble averaging has a different meaning from time averaging. It is a crucial difference for URANS. To understand ensemble averaging for, let us denote u as a component of velocity at a particular position and time in a repeatable turbulent flow experiment. Such variable will be necessarily random, and will be characterized by a probability distribution. Let us also denote $u^{(n)}$ as the n-th repetition of the experiment (or realization). These newly defined random variables will have the same probability distribution of *u*. Ensemble averaging will then be defined as the average over N realizations:

$$\langle u \rangle = \frac{1}{N}\sum_{i=1}^{N} u^{(n)} \tag{3}$$

Where the mean value of $\langle u \rangle$ corresponds to the mean value of *u*. Of course, time averaging does correspond to ensemble averaging in the sense that averaging over time corresponds to averaging over different realization of the flow field. In fact, in the present case we will consider steady flows, i.e., flows for which the principal characteristic of turbulence do not change in time when time averaged is performed over a sufficient amount of time.

However, if we limit conceptually ensemble averaging to a small amount of realizations, this equates to assuming that the flow is actually unstable since the turbulent statistics are allowed to fluctuate. Practically this is done by not considering the time derivate in (2.1) and (2.2). Then the velocity becomes a function of time $\langle u_i \rangle(t)$ and a time average needs to be considered to obtain the correct averaged value $\overline{\langle u_i \rangle}$. In this sense URANS becomes a sort of generalized filter (in time and

space) with characteristic filter lengths and filter times and it acts in much the same way as LES acts spatially.

Following this line of reasoning URANS is significant only when the fluctuation of $\langle u_i \rangle(t)$ is on time scales larger than the characteristic filter length and filter time. How to evaluate such lengths and times? This can be debated, but they are reasonably given by the particular turbulence model used for τ_{ij}. As an example, if a k-ε model is used to model the stresses a reasonable length-scale for the model will be given by $k^{3/2}/\varepsilon$, which is the usual time scale of isotropic turbulence.

Therefore a URANS simulation in a k-ε formulation will be significant only when fluctuations can be expected to deviate significantly from isotropic turbulence or mild anisotropy, i.e., when large-scale/ long-time coherent structures are present. Such cases are abundant in nuclear engineering where large-scale long time coherent structures determine the hydrodynamics in crucial parts of the reactor. Examples are rod-bundles and T-junctions:

1. Immediately downstream of the part where hot and cold water flows meet in T-junctions, temperature fluctuation of fluid arises, which repeatedly give a thermal load to structures ([1]). Some examples of damage due to thermal striping have been reported in mixing tees of the feedwater system, reactor water cleanup system and residual heat removal system in light water reactor (LWR) power plants. Since the high-cycle thermal fatigue phenomenon due to temperature fluctuation strongly depends on the geometrical form of the structure and the flow pattern, it is difficult to generalize an evaluation method from limited experimental results. A CFD-based methodology able to simulate this inherently unsteady phenomenon is therefore likable, in order to provide the necessary guidance to design and operation.
2. the flow in a tight rod bundle presents long-term, large scale coherent structures propagating in the streamwise direction [2]. At present, the contribution of these structures to mixing is not often considered, and no satisfying explanation for their presence has yet been provided.

In the following sections we will examine in detail these two cases. Let us first clarify two important points about URANS

Often the evaluation of the velocity is not sufficient for engineering purposes. Additional statistics such as the variance of the velocity components need to be considered. In URANS however the evaluation of such quantities needs to carefully considered. Let us take as an example the variance for the velocity components (but the same considerations could be extended to any other quantity) averaged over time.
It is possible to decompose the velocity in two components: the varying ensemble average and the fluctuations. This can be formalized in the following equation:

$$u_i(t) = \langle u_i \rangle(t) + u_i'(t) = \overline{\langle u_i \rangle(t)} + \left(\langle u_i \rangle(t) - \overline{\langle u_i \rangle(t)} \right) + u_i'(t) \qquad (4)$$

Which translates in the following equation for the variances:

$$Var(u_i) = \overline{\left(u_i - \overline{u_i}\right)^2} = \overline{\left(\langle u_i \rangle - \overline{\langle u_i \rangle}\right)^2} + \overline{\langle u_i'^2 \rangle} \tag{5}$$

The first component will define as coherent part, while the second needs closure since it depends upon the definition of the modeling [3] . The value of $\overline{\langle u_i'^2 \rangle}$ can in fact be derived from the model used for τ_{ij} .

In the present work the focus will be on k-ε models because of their popularity and widespread use, since an unsteady calculation can be time-consuming (and only a limited number of tests can be done). A complete description of the anisotropic k-ε formulation adopted for this work is available in [3]. The calculations have been performed with a quadratic or cubic formulation for the where the usual transport equations for the turbulent energy k and the turbulent dissipation rate ε are adopted [4]. In contrast with the standard model the adopted approach respects the constraint of realizability following the example of Lumley [5] which is reflected in formulation of the C_μ coefficient not being a constant but given as function of the shear invariant *S*.

For rod-bundles a quadratic algebraic relation for the stresses has been selected while, a cubic algebraic for the stresses has been used for T-junction. In fact, in both cases, secondary flows (related to the presence of anisotropic turbulence) are present and only non-linear k-e formulations are able to reproduce them.

For T-junctions the flow is also highly influenced by the curvature of the flow at the junction, which contributes significantly to the formation of secondary flows. The interaction between the Reynolds averaged stresses and curvature can be reproduced only with algebraic relations of order higher than three [6].

2. T-JUNCTION

The typical computational model used for CFD calculations ([7], [8], and [9]) of the flow in a T-junction is shown in Fig. 1. The model include two short inlet branches where the velocity is imposed and an outlet where the mass flux is imposed to equal to the sum of the two inlet fluxes.

Unsteady Reynolds Navier-Stokes methodologies do not need complex boundary formulations for the inlet but the outlet boundary condition presents computational problems in itself, and the outlet branch of the t-junction needs to be very long in order for the flow to develop properly. Following [8], in the present work the length has been selected to be equal to 20 times to diameter of the tube (in [8] the length of the branch was actually equal to 25 times the diameter of the pipes).

URANS has also been applied in several cases to the flow in a T-junction but the results were even less satisfactory than LES and DNS, especially in a case where buoyancy plays a dominant role [10]. This is an inherent limit of URANS that cannot be easily addressed. For buoyancy flows, LES/DNS methods remain the only reliable CFD methodology.

For cases where buoyancy is marginal however, there is no reason to assume that URANS would not be able to reproduce accurately the oscillatory behavior of the temperature. In fact, we will argue in the following that bad results obtained with URANS are to be imputed to an incomplete application of methodology.

In the present work we will simulate the experimental case Nr. 14 published in [11]. The case simulated was isothermal but the fluid in the two inlets was characterized by different conductivity. Thus the mixing can be adequately modeled by the solution of a transport equation for an arbitrary passive scalar. The choice of the experiment is motivated by:

1. the absence of buoyancy;
2. the detailed rms (root mean square) plots published by the authors, which permit an assessment of the capability of the code to correctly reproduce the rms of the passive scalar;
3. the high resolution.

The diameter of the tube is equal to 0.05 m, the working fluid is water and the Reynolds number on both inlet branches is equal to 25000.

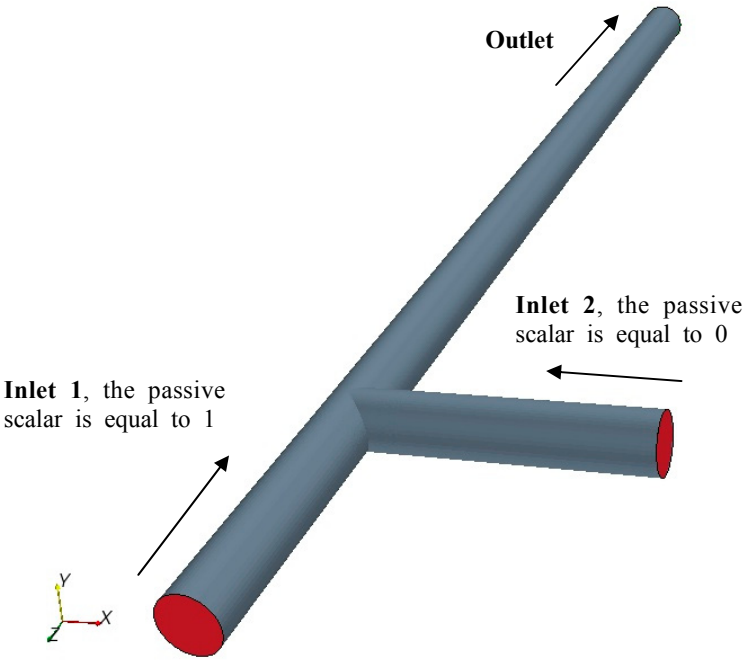

Fig. 1 Computational Model

2.1 Model

In order to model the mixing in the T-junction and additional equation is solved for the concentration *c* of high conductivity fluid. This concentration ranges between 0 (at the inlet of the low conductivity fluid) to 1 (at the inlet of the high conductivity fluid). The Transport equation for the passive scalar c can then be written (in a URANS approach) as:

$$\frac{\partial\langle c\rangle}{\partial t}+\langle u_j\rangle\frac{\partial\langle c\rangle}{\partial x_j}=-\frac{\partial}{\partial x_j}\left(\tau_j^c-\frac{\nu}{\sigma}\frac{\partial\langle c\rangle}{\partial x_j}\right) \tag{6}$$

Where σ is the Schmidt number of the fluid and $\tau_j^c=\langle cu_j\rangle-\langle c\rangle\langle u_j\rangle$, which represents a term that needs closure. The following model is usual employed:

$$\tau_j^c=-\frac{\nu_t}{\sigma_t}\frac{\partial\langle c\rangle}{\partial x_j} \tag{7}$$

Where $\nu_t=\frac{\mu_t}{\rho}$ and σ_t is the turbulent Schmidt number for the fluid. Since the objective of the present work is to predict correctly not only the correct value of the concentration but also the fluctuations, it is necessary to evaluate the rms of the concentration. Following what outlined in the introduction, the rms can be defined as:

$$c_{rms}^2=\overline{\left\langle\left(c-\langle c\rangle\right)^2\right\rangle}+\overline{\left(\langle c\rangle-\overline{\langle c\rangle}\right)^2} \tag{8}$$

where the overbar here represents the operation of averaging over time. The second term (coherent) takes into account the contribution to the fluctuation of c given by large scale structures, i.e. the turbulent structures that are simulated though the URANS simulation. The first term (incoherent) is related to the c contribution to the fluctuation of c given by the inherent nature of turbulence. The evaluation of the first term can be carried out only through the solution of an additional equation for the transport for the variance of the scalar c. This equation assumes the shape [12]:

$$\frac{\partial\langle c'^2\rangle}{\partial t}+\langle u_j\rangle\frac{\partial\langle c'^2\rangle}{\partial x_j}=-\frac{\partial}{\partial x_j}\left(\tau_j'^c-\frac{\nu}{\sigma}\frac{\partial\langle c'^2\rangle}{\partial x_j}\right)+P-D \tag{9}$$

where $\overline{\langle c'^2\rangle}=\overline{\left\langle\left(c-\langle c\rangle\right)^2\right\rangle}$. $\tau_j'^c$ can be modeled in fashion similar to τ_j^c. P is the production term and D is the dissipation term for the variance of the scalar. P is defined as :

$$P = -2\tau_j'^c \frac{\partial \langle c \rangle}{\partial x_j} \tag{10}$$

and therefore can be directly computed. The dissipation term D can be traditionally model, in equilibrium flows, through:

$$D = C_\chi \frac{\varepsilon}{k} \langle c'^2 \rangle \tag{11}$$

C_χ has been chosen to be equal to 1.5 following Warhaft [13]. Since, however the flow in the junction area is not in equilibrium (i.e., turbulence is not isotropic), this model might not be particularly accurate. Possible improvements over this model might need to be considered.

The code used is STAR-CD 4.06 [12].

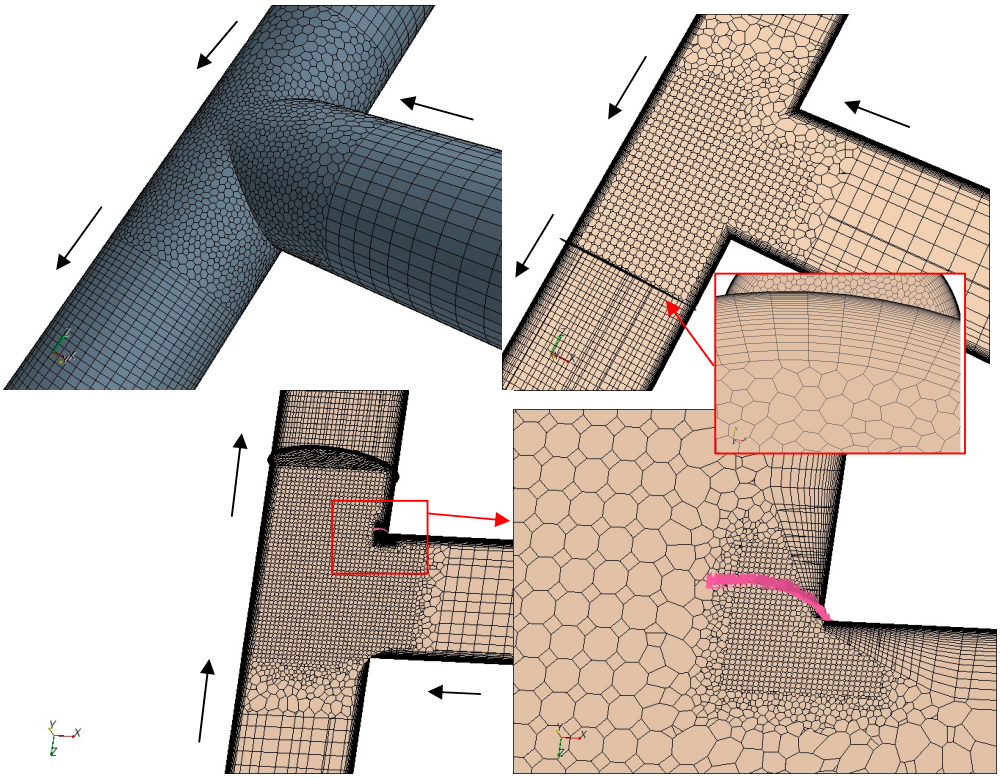

Fig. 2 Coarse Mesh (Top) and Fine mesh (Bottom).

A polyhedral grid has been used with a prismatic layer near the wall boundary. The wall region has been modelled through a Low-Reynolds model. Two different meshes have been used, a fine grid (approximately 1,000,000 polyhedral meshes) and a coarse grid (approximately 500,000 polyhedral meshes). Images of the meshes are shown in Fig. 2. Steady state calculations have been run on both meshes. Since the difference

between the results was not significant, the URANS calculation has been run only on the coarse grid. The convective fluxes have been discretized through MARS (Monotone Advection and Reconstruction Scheme) [14]. Time advancement has been carried out in through implicit first order schemes with a CFL around 1.0. The algorithm used was PISO (Pressure Implicit with Splitting of Operators) which proved particularly apt to URANS calculations. The inlet boundary has been implemented by imposing the wall law for pipe flow at the inlets.

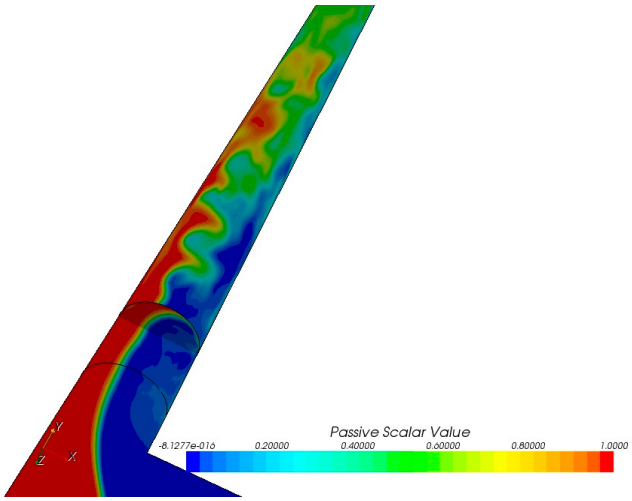

Fig. 3 Instantaneous contour plot for the passive scalar

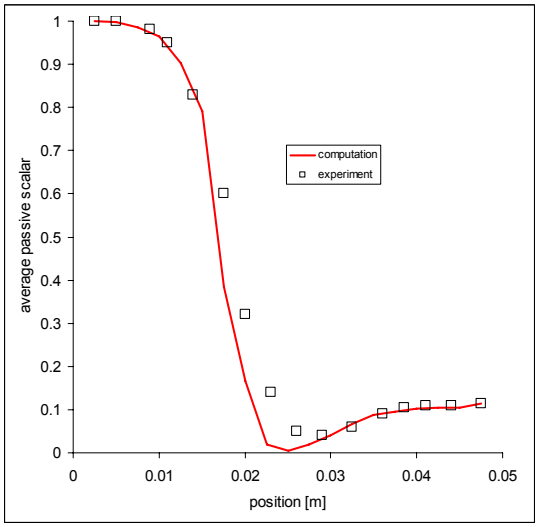

Fig. 4 Averaged for the passive scalar on the symmetry axis of the measurement plane

2.2 Results for the scalar

The instantaneous distribution of the passive scalar reflects the presence of coherent structures downstream of the junction (**Figure 3** shows a section on the plane parallel to the streamwise direction for an instantaneous plot of the passive scalar).

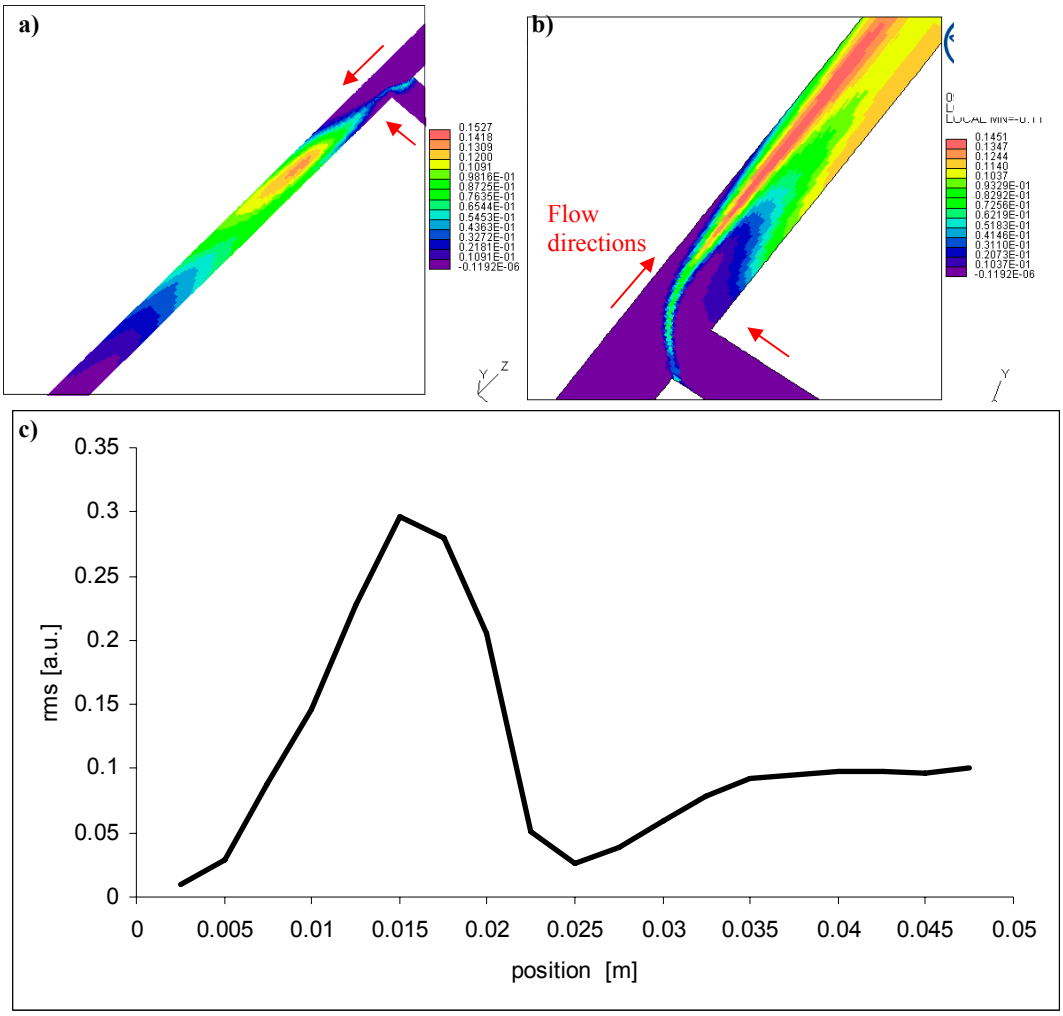

Fig. 5 (a) Averaged variance for the passive scalar on the wall and (b) section plot on the symmetry plane and (c) Rms of the scalar on the symmetry axis of the measurement plane

In fact, it is possible to notice that the passive scalar presents a strong oscillating behaviour downstream of the junction, which is indicative of strong vertical structures. When Reynolds averaged is applied to the passive scalar the distribution of the scalar presents a sharp interface between the mixing fluids, up to 3 D downstream of the junction. Interestingly enough however in the vortex region (the region closer to Inlet 2), the averaged value of the scalar is higher than 0 in the near wall region. This suggests that part of fluid from Inlet 1 is entrained in the vortex region from further downstream [11]. For the passive scalar the authors of [11] published detailed

experimental results therefore it was possible to give a comparison on the measurement plane. These results are given in Fig. 4.

Accuracy is deemed acceptable except in the interface region where, possibly, the resolution might be insufficient to fully capture the dynamics of the interface. It is also possible that the ensemble average time in the experiment was not sufficient.

2.3. Results for the rms

The authors of [11], published also a contour plot of the rms of the passive scalar on the measurement plane. The peak value of the rms on the measurement plane was found approximately equal to 0.33 m/s. As discussed in the previous sections, the only way to correctly simulate the rms of the passive scalar is to consider both contributions to the variance. This has been done in STAR 4.06 though the use of user subroutines. The averaging in this case has been performed over 2 s and 20.000 time steps. As it is possible to see from Fig. 8, the computed rms on symmetry line of the measurement plane is equal to 0.3. Thus reasonably close to the experimental value. The distribution of the rms is also in qualitative agreement with the experiment: the position of the rms peak is approximately 0.008 m from the centre of the outlet pipe in the calculation and approximately 0.007 m in the experiment (value extrapolated from the contour graph).

This agreement can be achieved only if both contributions to the variance in equation (8) are included. Any implementation of URANS which disregards one of the components would immediately feature an error on the variance of 25 % (by a steady state calculation for example) or 75 % (by not simulating the equation for the variance of the scalar).

3. TIGHT ROD-BUNDLES

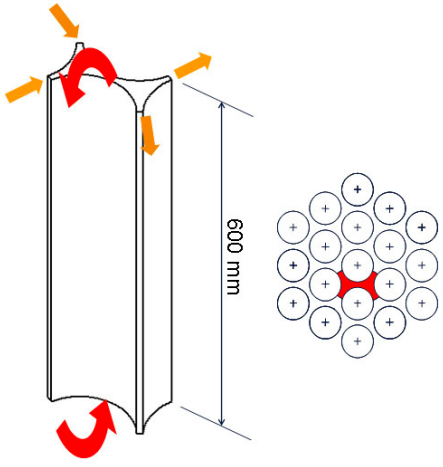

Fig. 6 Geometry and boundary conditions

The actual flow in a rod bundle is neither steady nor stable; in fact it presents long-term, large-scale coherent patterns in the axial direction that are evident when the P/D

ratio is small. The contribution of these structures cannot be taken into account by a steady state simulation, unless specific ad-hoc models are introduced in the momentum equations. Since these models are not available, and their accplicability is disputable, a fully transient simulation is believed to be necessary.

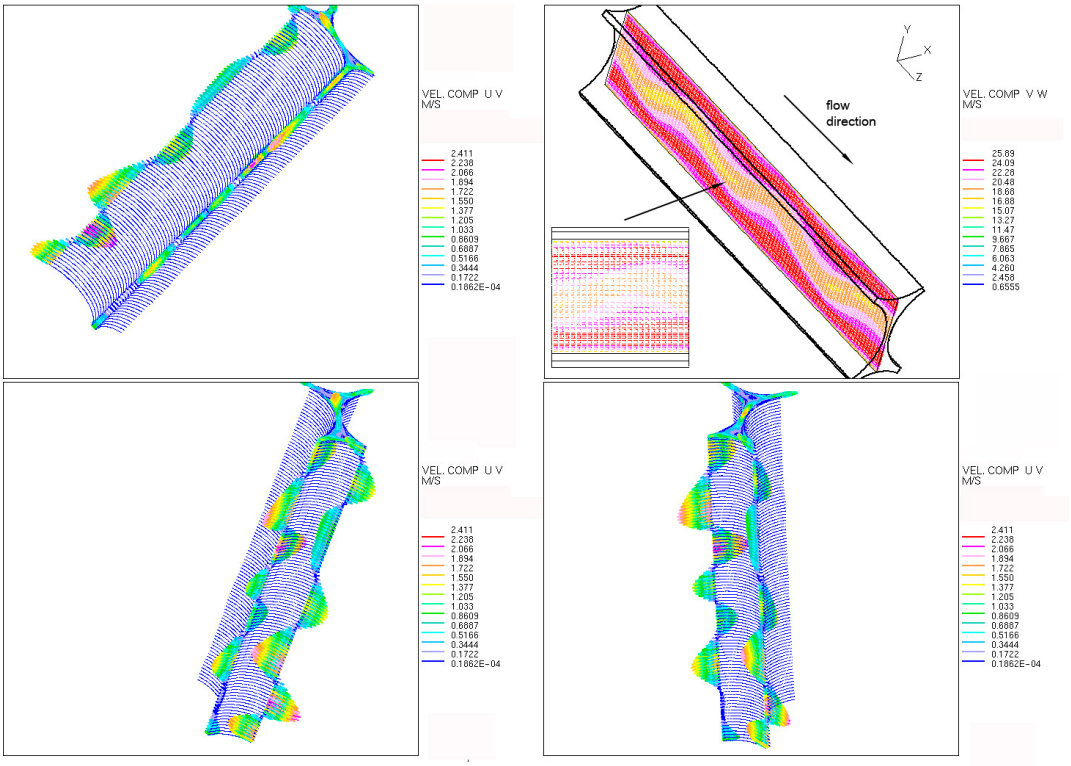

Fig. 7 URANS simulation of the flow in a rod bundle (details are available in [1], an infinite rod-bundle is modelled as two channels with periodic boundary conditions in the cross section

Indications of an unusual behavior of the flow in rod bundles are known since the works of Coates [15], Moyer [16], Todreas [17]. The high mixing coefficient between sub-channels measured by these authors could not in fact be accounted by the sole turbulent diffusion [18]. Actual evidence of large scale structures goes back to the fundamental studies of Hooper and Rehme [19], where the authors observed an oscillatory behavior for the cross velocity in the narrow gap of a two sub-channel experiment. Several other geometries have been investigated over the years, i.e. a triangle lattice assembly of cylindrical pins with a P/D of 1.06 ([2]), a series of rectangular channels layouts [20], [21], and other simplified concepts [22].

Numerical simulations of tight fuel bundles should ideally be able to reproduce these important structures. Attempts to simulate the oscillation in a CANDU-type rod-bundle [22] have been quite successful from the point of view of averaged statistics such as the turbulent intensity and the streamwise velocity. Other simulations, concerned with simpler geometry layouts have also achieved some success.

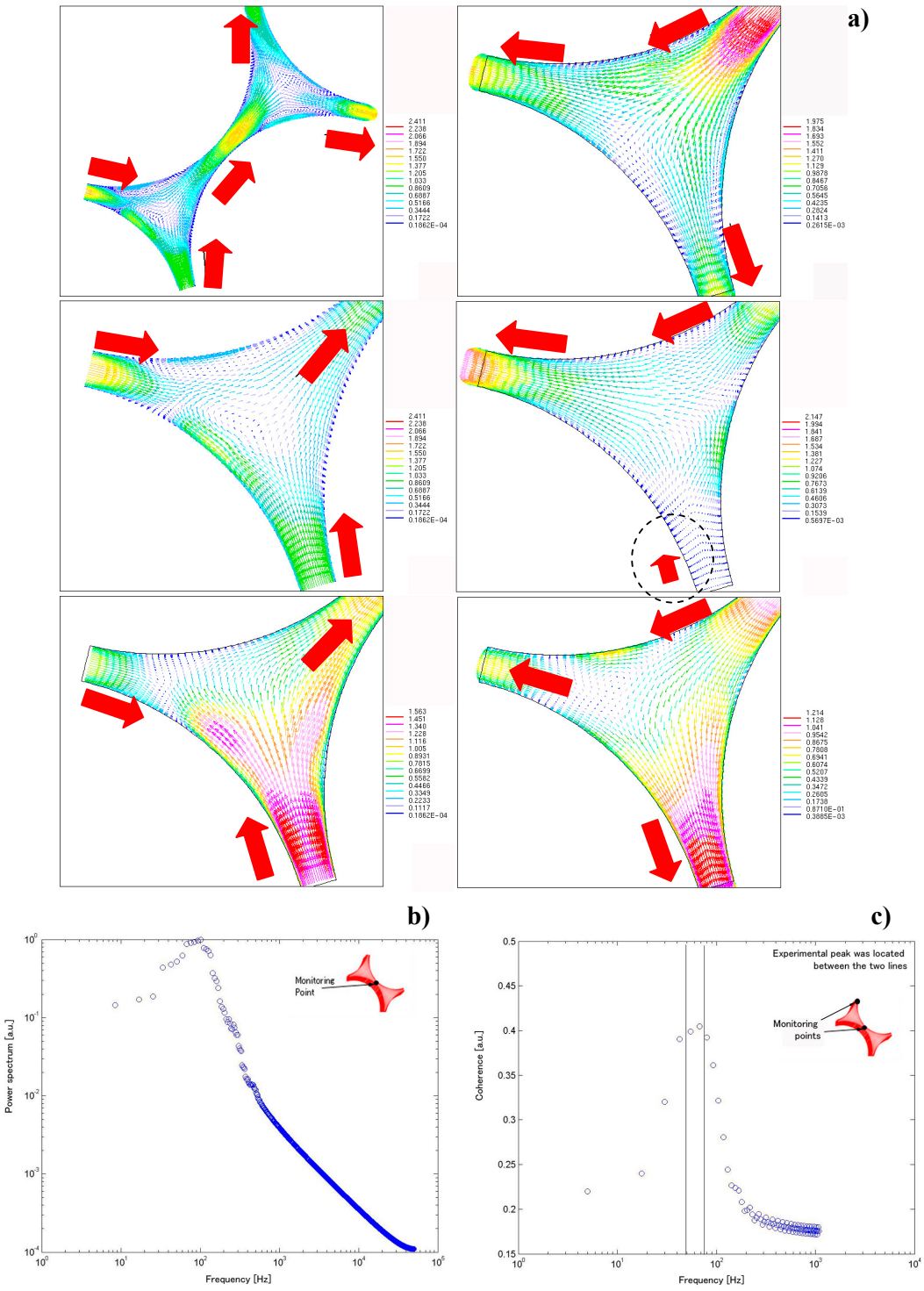

Fig. 8 URANS simulation of the flow in a rod bundle: interaction between the oscillation in different gaps (a) power spectrum in the central gap (b) coherence function (c)

In the present simulation the focus will be on the experimental setup of Krauss and Meyer ([2]). In particular we will refer to the case characterized by the following:

1. a Reynolds number of 38,754;
2. a hydraulic diameter of 33.5 mm;
3. a P/D of 1.06;
4. the working fluid has a viscosity of 1.9194×10^{-5}.

The grid employed is rather fine (over 600,000 meshes for the Low Reynolds formulation about 300,000 if wall functions are used); the computational model is shown in Fig. 6. The PISO (Pressure Implicit with Splitting of Operators) algorithm along with an Euler implicit time advancement scheme and a QUICK (Quadratic upstream interpolation of convective kinematics) spatial discretization has been used in STAR-CD 3.26. Since periodic boundary conditions are used in the cross section and the streamwise direction special attention needs to be paid to the length of the domain [24] (in the present case it has been chosen to be equal to 600 mm).

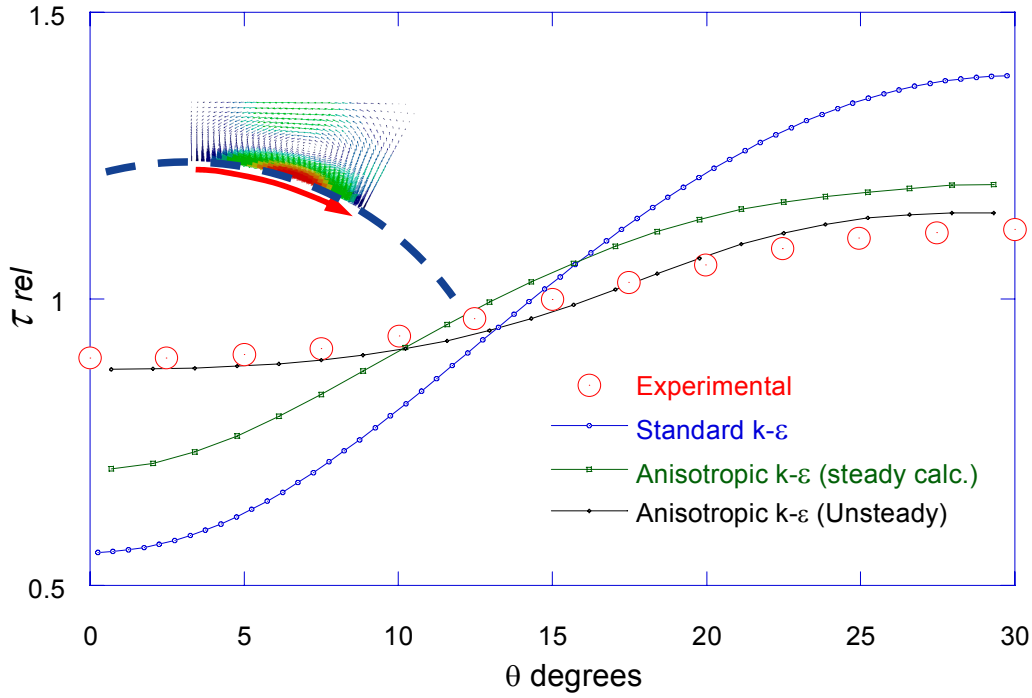

Fig. 9 Wall shear stress

Fig. 7 shows the coherent structures as they develop on boundaries and in a section of the domain. They constitute a truly three-dimensional pulsation. The cross velocity in each narrow gap has a sinusoidal behavior and a characteristic power spectrum. The interaction between the oscillations in different gaps is complex (Fig. 8), but the oscillations are not in phase. As a matter of fact the coherence function between different gaps fits well the experimental counterpart and it is peaked at a value slightly smaller than the peak of the power spectrum. The correct reproduction of the oscillations ensures that the averaged statistics are well represented as well. The use of an unsteady simulation allows for a strong improvement in accuracy. It is particularly evident observing the wall shear stress (Fig. 10). If the error in a steady state case simulation using the anisotropic model arrived at 20 %, here the agreement using the same model is excellent. Fig. 10 shows the dependence of the wall shear

stress on the angle.

Another important feature of the flow in rod bundles is the presence of secondary flows in the cross section. As mentioned in Baglietto [3], the quadratic anisotropic model adopted is able to capture the secondary flows in a steady-state simulation. In an URANS, however, the symmetry of the flow is instantaneously broken, and it is not possible to observe any coherent pattern if averaging is performed over a short integration time. This is an inherent characteristic of URANS: since it simulates part of turbulence (i.e., the part corresponding to larger scales) it needs a considerable time to achieve convergence of the statistics. However, when Reynolds averaging is performed over a sufficient integration time it is possible to recover the shape of the secondary flows (Fig. 10).

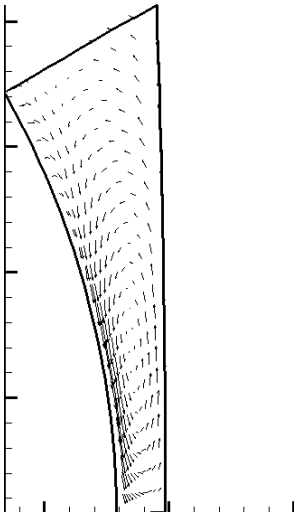

Fig. 10 Averaged Secondary flows (Integration time of 1s)

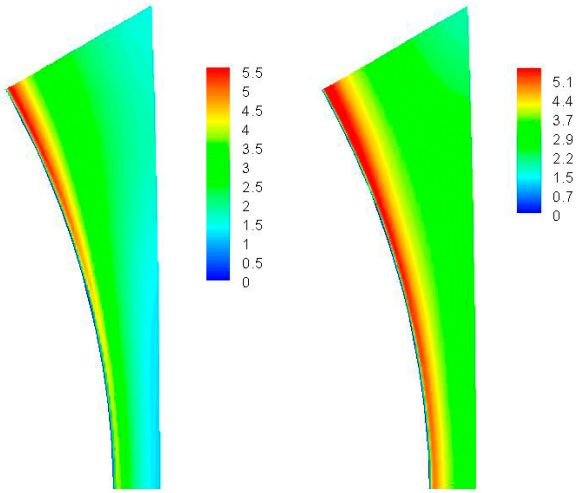

Fig. 11 Turbulent intensity (not normalized): left, modeled component; right, overall turbulent intensity

As for the turbulent intensity, extensive data is provided only far from the wall. We report an isoplot in Fig. 11 for the un-normalized turbulent intensity:

$$k = \frac{1}{2}\left(\overline{\langle u'^2 \rangle} + \overline{\langle v'^2 \rangle} + \overline{\langle w'^2 \rangle}\right), \tag{12}$$

where u is the streamwise velocity, v the radial velocity and w the azimuthal velocity. Normalizing through the friction velocity it is possible to obtain

$$k^+ = \frac{1}{u_\tau^2} k + \frac{1}{u_\tau^2} \sum_i \left(\langle u_i \rangle - \overline{\langle u_i \rangle}\right)^2 . \tag{13}$$

For such quantity the agreement with the experiment [2] is excellent as given in [24].

4. CONCLUSIONS

The use of URANS for two important classes of flows for nuclear engineering has been considered. In both cases, it has led to a considerable improvement over steady state calculations. In particular:

1. For T-junctions, A scalar equation has been solved to model the mixing in the junction region. This model corresponds to the mixing of a hot fluid and a cold fluid whenever buoyancy plays a marginal role. The methodology was able to reproduce at least qualitatively the flow field. It has been demonstrated that without including an additional transport equation for the variance of the scalar, URANS is unable to predict the correct value of the rms of the scalar. This result is relevant to the prediction of thermal fatigue, since the rms of the temperature in the near wall regions of the pipe is an important physical
2. An URANS simulation of the flow in a tight lattice rod-bundle has been carried out. The coherent structures have been simulated successfully After comparing the results obtained through URANS and RANS, it has been concluded that, in experimental conditions where oscillations are present, unsteady simulations are necessary if accuracy in the prediction of averaged statistics is needed.

This works represent a step toward a general approach for the prediction, throu gh CFD tools, of the flow in arbitrarily chosen rod-bundles and other flows wh ere large-scale coherent structures dominate the hydrodynamics.

REFERENCES

1. T. Kawamura et al., “Experimental study on thermal striping in mixing tees with hot and cold water”, ICONE 10, April 14-18, 2002
2. T. Krauss, L. Meyer, “Experimental investigation of turbulent transport of momentum and energy in a heated rod bundle”, *Nuclear Engineering and design*, **Vol. 180**, pp. 185-206 (1998)
3. E. Baglietto and H. Ninokata, “Anisotropic Eddy Viscosity Modeling for

Application to Industrial Engineering Internal Flows", *Int. J. Transport Phenomena*, **Vol. 8**, n. 2 (2006)

4. B.E. Launder and D.B Spalding, "The numerical computation of turbulent flows", *Comp. Meth. in Appl. Mech. and Eng*.,**Vol.** 3, pp. 269-289 (1974)
5. J. L. Lumley, "Toward a turbulent constitutive relation*", J. Fluid Mechanics*, **Vol. 41**, pp. 413-434 (1970)
6. D. D. Apsley and M. A. Leschziner, "A new low-Reynolds-number nonlinear two-equation turbulence model for complex flows**",** *International Journal of Heat and Fluid Flow*, **19**, pp. 209-222 (1998)
7. N. Fukushima, K. Fukugata, N. Kasagi, H.Noguchi, K. Tanimoto, "Numerical and Experimental Study on Turbulent Mixing in a T-junction Flow", 6th Joint ASME-JSME Thermal Engineering Joint Conference, March 16-20, 2003
8. A.K. Kuczaj, B. de Jager and E. Komen, "An assessment of Large-Eddy Simulation for thermal fatigue Prediction", ICAPP, United States, 2008
9. Hu, L.W., Kazimi, M.S., "Large Eddy Simulation of Water Coolant Thermal Striping in a Mixing Tee Junction," NURETH-10, Seoul, Korea, October 5-9, 2003
10. J. Westin et al. "Experiments and Unsteady CFD-Calculations of Thermal Mixing in a T-Junction", CFD4NRS, Garching, 5-7 September, 2006
11. R. Zboray, A. Manera, B. Niceno and H.M. Prasser, "Investigations on Mixing Phenomena in Single-Phase Flows in a T-junction Geometry", Nureth-12, Pittsburgh, Sept. 30-Oct. 4, 2007
12. K. J. Hsieh, F. S. Lien and E. Yee, "Numerical modeling of passive scalar dispersion in an urban canopy layer", *Journal of Wind Engineering and Industrial Aerodynamics***, 95**, 1611, (2007)
13. Z. Warhaft, "Passive scalars in turbulent flows", *Annu. Rev. Fluid Mech.* **32**, 203–240, (2000)
14. STAR-CD 4.06 Methodology Guide
15. D.E. Coates, "Interchannel mixing and cooling temperature distribution in seven and nineteen element fuel bundles", **X07-10001R**, Canadian General Electric Company Ltd. (1960)
16. C.B. Moyer, "Coolant mixing in multirod fuel bundles", *Riso report*, **No. 125**, July 1964
17. N.E. Todreas,"Coolant mixing in sodium cooled fast reactors fuel bundles", **WASH-1096** (1968)
18. V. R. Skinner, A. R. Freeman and H. G. Lyall, " Gas mixing in rod clusters", *Internal Journal of Heat and Mass transfer*, **Vol. 12**, pp. 265-278, (1969)
19. J.D. Hooper, K. Rehme, "Large-Scale structural effect in developed turbulent flows through closely-spaced rod arrays", Journal *of Fluid Mechanics*, **Vol. 145**, pp. 305-337 (1984)
20. A. Lexmond, M. Mudde, T.J.J. Van der Haagen, "Visualization of the vortex street and characterization of the cross flow in the gap between two subchannels", *11th Nureth*, Avignon, France (2005)
21. L. Meyer, K. Rehme, "Large-Scale Turbulence Phenomena in Compound Rectangular Channels", *Experimental Thermal and Fluid Science*, **Vol. 8**, pp. 286-304 (1994)
22. M.S. Guellouz, S. Tavoularis, "The structure of Turbulent flow in a rectangular channel containing a cylindrical rod – Part 1: Reynolds averaged experiments",

Experimental Thermal and Fluid Science, **Vol. 29**, pp. 59-73 (2000)

23. D. Chang, S. Tavoularis,"Numerical simulation of turbulent flow in a 37-rod bundle", *Nuclear Engineering and Design*, **Vol. 237**, pp. 575-590 (2007)
24. E. Merzari, E. Baglietto, H. Ninokata, "Numerical Simulation of the flow in Tight-Lattice Fuel Bundles", Nuclear Engineering and Design, **238**, pp. 1703-1719 (2008)